Supplementary Methods:

Animals

The genetic mouse models used in this study are summarized in Online Table I. 4033 MCAT mice were originally derived in the C57BL/6J background[2] but were subsequently backcrossed to C57BL/6NCrl. The floxed stop sequence preceding mCAT in the inducible BAC model of expression was excised by tamoxifen induced Rosa26 or MHC promoted Cre (Online Fig I). All mouse strains were shown to have wild type nicotinamide nucleotide transhydrogenase by Western blot. All animal experiments were approved by the University of Washington Institutional Animal Care and Use Committee. Mice were housed in a barrier specific-pathogen-free facility and maintained as described[2].

Primary mouse neonatal ventricular cardiomyocyte culture, flow cytometry and confocal microscopy

Hearts from 24-72h postnatal C57Bl6/FVB mice were dissected, minced, and enzymatically isolated with Blendzyme 4 (45 µg/ml, Roche). Following enzymatic digestion, cardiomyocytes were enriched using differential pre-plating for 2h, then seeded on fibronectin-coated culture dishes for 24h in DMEM (Gibco), 20% Fetal Bovine Serum (Sigma), and 25 µM arabinosylcytosine (AraC; Sigma) to inhibit non-cardiomyocyte proliferation. Cardiomyocytes were then stimulated with Ang (1µM) for 2 h in serum-free culture medium containing 0.5% insulin-transferrin-selenium (Sigma), 3mM Na-pyruvate, 2 mM glutamine and 1mg/mL of BSA. Cardiomyocytes were loaded with Mitosox (5µM), Dihydroethidium (DHE,

5□m), Dihydrochlorofluorescein (DCFDA, 5μM), or tetramethylrhodamine ethyl ester (TMRE, 10mM) for 30 min at 37ºC, followed by 2 washes with Hanks Balanced Salt Solution. Flow cytometry was performed as previously described[3] using excitation/emission of 488/625 nm for Mitosox and DHE and 488/525 for DCFDA. Data analysis was performed using FCS Express (De Novo Software, Los Angeles, CA).

Confocal microscope images were collected on a Zeiss 510 Meta using the Zeiss LSM software. Images of MitoSOX fluorescence were obtained using a 63X Oil objective with an excitation at 514nm and an emission of 560-615nm. Images of TMRE were obtained using excitation at 568nm and an emission of 590-630 nm. Quantitative analysis of total cellular fluorescence of 11-13 fields from duplicate wells was performed using NIH Image J.

Angiotensin II, AZT delivery, Echocardiography and Blood Pressure Measurement.

Four to seven male mice were included in each experimental group. Ang (1.1 mg/kg/d) was continuously infused over a 4 week period using an Alzet 1004 osmotic minipump implanted subcutaneously over the dorsal thorax.

Comparison of blood pressure response to Ang in WT, pCAT and mCAT mice was measured by continuous blood pressure telemetry using intravascular catheter PA-C10 (Data Science International [DSI], MN), in which measurements were taken every three hours starting from 2 days before until 2 days after Ang pump emplacement. AZT (240 mg/kg/d) was added to drinking water and fresh

AZT water was administered every week for 8 weeks. Echocardiography was performed at baseline and at the end of experiments as described using Siemens Acuson CV-70 equipped with 13MHz probe[4]. Briefly, isoflurane 0.5% mixed with O_2 was used to provide adequate sedation but minimal cardiac suppression during echocardiography. M-mode, conventional and Tissue Doppler, and functional calculations were performed according to American Society of Echocardiography guidelines. An increase in MPI (calculated as the ratio of the sum of isovolemic contraction and relaxation time to LV ejection time) indicated that a greater fraction of systole was spent to cope with the pressure changes during isovolemic phases, and has been shown to reflect both LV systolic and diastolic dysfunction [5].

Measurement of mitochondrial protein carbonyl groups

LV tissues were homogenized in mitochondrial isolation buffer (sucrose 250mM, 1mM EGTA, 10mM HEPES, 10mM Tris-Hcl, pH7.4), then the lysates were centrifuged at 800g for 10 minutes. The supernatants were further centrifuged at 4000 g for 30 min at 4ºC. The crude pellets were then resuspended in small volume of isolation buffer, sonicated on ice and treated with 1% streptomycin sulfate to precipitate mitochondrial nucleic acids. One µg/assay was analyzed using a ELISA kit based on derivatization of the carbonyl group with dinitrophenylhydrazine (DNPH), followed by anti-DNPH antibody (OxiSelect protein carbonyl ELISA, Cell Biolabs, San Diego, CA). To examine the purity of mitochondrial extract, we performed Western blots using antibodies for

mitochondrial protein Prohibitin (Biomeda Corp, 1:1000) and cytosolic protein GAPDH (Millipore,1:10,000) (Online Fig. III)

The random mutation capture assay was used to detect both the common deletion and random deletions located between two PCR primers, and was performed as previously described[4]. The RMC assay was employed as it is able to detect one mutant molecule in 10^7, in contrast to the sensitivity by conventional gel electrophoresis, which is one part in 10^2 to $10^{3\,6}$. In brief, a crude mitochondrial fraction is isolated followed by mtDNA purification and mtDNA digestion with TaqI endonuclease. Real-time PCR was performed with two primer sets. The first set (deletion primers) flanked multiple TaqI restriction sites several kb apart and was amplified only if there was a segmental deletion of all TaqI restriction sites which rendered the DNA molecule resistant to Taq I cleavage. The second set (controls) amplified an adjacent region not containing a TagI restriction site, and quantitated the total amount of mtDNA template in the sample. Using a comparative PCR-strategy, WT and mutant molecules were quantified, and the amount of mutant molecules was normalized to the amount of WT molecules in order to calculate the deletion frequency. The primers for deletion assay were AGGCCACCACACTCCTATTG and AATGCTAGGCGTTTGATTGG, and the control forward and reverse primers were TCGGCGTAAAACGTGTCAACT & CCGCCAA GTCCTTTGAGTTT, respectively.

Quantitative PCR

The quantitation of relative gene expression was performed using Taqman Gene Expression Assays and a Applied Biosystems 7900 thermocycler. The genes include: PGC1-α (Mm00731216), TFAM (Mm00447485), NRF-1 (Mm00447996), NRF-2 (Mm00487471), ANP (Mm01255747), BNP (Mm 00435304) and collagen 1a2 (Mm 00483937). All expression assays were normalized to 18S RNA.

Mitochondrial DNA copy number was quantified using quantitative PCR of total DNA extracts from cardiac tissues. Mitochondrial DNA copies were estimated by the ratio of the amount of mitochondrial gene NADH dehydrogenase 1 (ND1) and a single-copy nuclear gene cytochrome P4501A1 (cyp1A1), as previously described[4].

Transmission Electron Microscopy

Electron microscopy was performed on a JEOL JEM 1200EXII transmission electron microscope at 15,000X. Quantitative analysis of damage mitochondria and autophagosomes was quantified blindly from 8-10 images from different fields (15,000x magnification). Damaged mitochondria were defined by vacuolation (loss of electron density) or disrupted cristae. Autophagosomes or autolysosomes were identified by the characteristic structure of a double or multi-lamellar smooth membrane completely surrounding compressed mitochondria or membrane bound electron-dense material[7].

Mitochondrial respiratory function

Saponin-permeabilized cardiac fibers isolated from the left ventricle were used to measure respiratory function of the total mitochondrial population in situ, as described [8]. Briefly, 15-25 mg of fresh left ventricular apex was dissected in cold Biops buffer (in mM: CaK_2 EGTA 2.77, K_2 EGTA 7.23, Na_2 ATP 5.77, $MgCl_2$ 6.56, taurine 20, Na_2 PCr 15, imidazole 20, DTT 0.5 and MES 50, with pH 7.1), followed by saponin permeabilization (50µg/mL) on ice for 35 minutes. The permeabilized cardiac fibers from the left ventricular apex were washed twice with Reaction buffer (in mM: mannitol 110, Tris 60, $MgCl_2$ 5, KH_2PO4 10, KCl 60, Na_2 EDTA 0.5 and 0.1% of BSA, pH: 7.4), then quickly blotted on filter paper, and inserted into the respirometry chamber (Oxygraph, Oroboros Instruments, Austria) containing 3ml Reaction buffer. Baseline respiration was collected for 20 minutes. ADP (1mM) and pyruvate (10 mM) and malate (6 mM) were added to induce state 3 respiration. State 4 respiration was measured after the addition of Oligomycin (1µg/mL). Respiration was measured at 25°C using a high resolution Oroboros oxygraph with all values corrected for atmospheric pressure during the experiment. Data collection and analysis was performed using LabView software.

Western blot

Antibodies for the Western blots are as following: anti LC-3 (Novus Biologicals, 1: 1000), anti p47phox (Santa Cruz Biotechnology, SC-14015, 1:1000), anti NOX4 (Santa Cruz Biotechnology, 1:1000), anti phospho-ERK1/2 (Millipore, 1:500

dilution), anti ERK1/2 (Cell Signaling, 1:250), anti-human erythrocyte catalase (Athens Research & Technology 01-05-030000, 1:1000) or mouse anti-cytochrome c (Mitosciences MSA06, 1:1000) and Donkey anti-rabbit secondary antibody (Thermo Scientific, 1:10000 dilution). To study p47phox membrane translocation (NOX2 activation), we performed subcellular fractionation. Briefly, 15-25 mg heart tissue pieces were homogenized in 400µl cold isolation buffer (sucrose 250mM, 1mM EGTA, 10mM HEPES, 10mM Tris-Hcl, pH7.4). The homogenate was centrifuged at 800g for 10 minutes. The supernatant was collected and further centrifuged at 100,000g for 40 minutes. The supernatant was collected as the cytosolic fraction, and the membranous pellet was resuspended in 30µl lysis buffer.

Immunohistochemistry

Cardiac tissue was fixed in 4% paraformaldehyde overnight at 4°C, followed by paraffin embedding and deparaffinization immediately before use. Sodium citrate buffer at 99°C was used for antigen retrieval. After blocking in bovine serum albumin, slides were stained with rabbit anti-human erythrocyte catalase (Athens Research & Technology 01-05-030000, 1:50) or mouse anti-cytochrome c (Mitosciences MSA06, 1:50) or mouse anti-myosin heavy chain (Millipore 05-716, 1:10), followed by goat anti-mouse Alexa 568 (Invitrogen A-21134, 1:100) and goat anti-rabbit Alexa 633 (Invitrogen A-21071, 1:100) for secondary and DAPI for nuclear stain. Images were visualized on a Leica Meta 510 Confocal microscope (Online Figure II).

Statistical Analysis

All data were presented as means ± SEM. Comparisons between two groups were performed using Student t-tests. One-way ANOVA was used to compare differences among multiple groups, followed by Tukey post-hoc test for significance. $P<0.05$ was considered significant.

References:

1. Luderer U, Kavanagh TJ, White CC, Faustman EM. Gonadotropin regulation of glutathione synthesis in the rat ovary. *Reprod Toxicol.* 2001;15:495-504.
2. Schriner SE, Linford NJ, Martin GM, Treuting P, Ogburn CE, Emond M, Coskun PE, Ladiges W, Wolf N, Van Remmen H, Wallace DC, Rabinovitch PS. Extension of murine life span by overexpression of catalase targeted to mitochondria. *Science.* 2005;308:1909-1911.
3. Mukhopadhyay P, Rajesh M, Hasko G, Hawkins BJ, Madesh M, Pacher P. Simultaneous detection of apoptosis and mitochondrial superoxide production in live cells by flow cytometry and confocal microscopy. *Nat Protoc.* 2007;2:2295-2301.
4. Dai DF, Santana LF, Vermulst M, Tomazela DM, Emond MJ, MacCoss MJ, Gollahon K, Martin GM, Loeb LA, Ladiges WC, Rabinovitch PS. Overexpression of catalase targeted to mitochondria attenuates murine cardiac aging. *Circulation.* 2009;119:2789-2797.
5. Tei C, Nishimura RA, Seward JB, Tajik AJ. Noninvasive Doppler-derived myocardial performance index: correlation with simultaneous measurements of cardiac catheterization measurements. *J Am Soc Echocardiogr.* 1997;10:169-178.
6. Vermulst M, Wanagat J, Kujoth GC, Bielas JH, Rabinovitch PS, Prolla TA, Loeb LA. DNA deletions and clonal mutations drive premature aging in mitochondrial mutator mice. *Nat Genet.* 2008;40:392-394.
7. Teckman JH, An JK, Blomenkamp K, Schmidt B, Perlmutter D. Mitochondrial autophagy and injury in the liver in alpha 1-antitrypsin deficiency. *Am J Physiol Gastrointest Liver Physiol.* 2004;286:G851-862.
8. Kuznetsov AV, Veksler V, Gellerich FN, Saks V, Margreiter R, Kunz WS. Analysis of mitochondrial function in situ in permeabilized muscle fibers, tissues and cells. *Nat Protoc.* 2008;3:965-976.

Online Supplement Material: Dai, et al

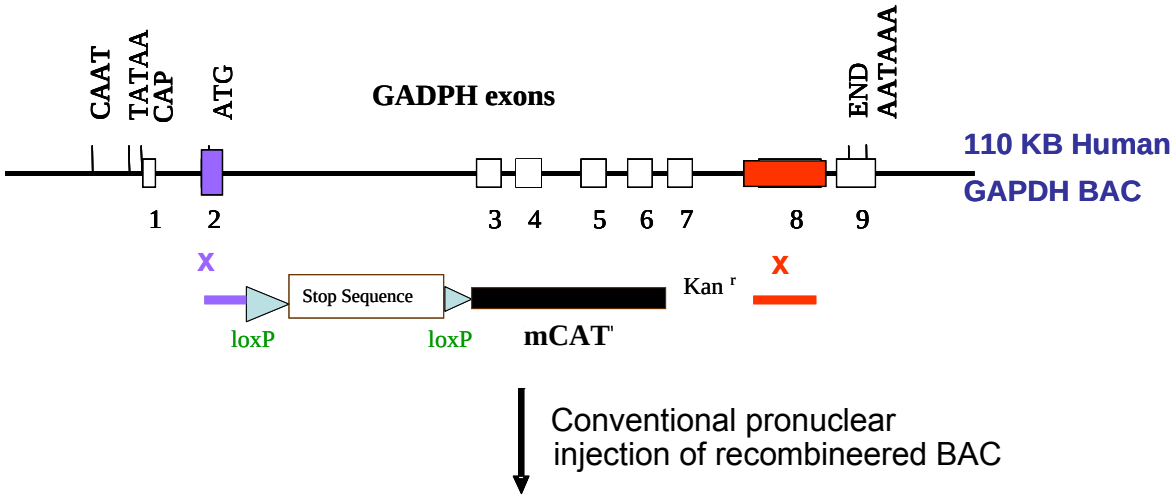

Online Figure I. Construction of the flox-stopped mCAT BAC mouse model. The mCAT sequence (8) was preceded by a stop sequence flanked by loxP sites, as previously described (Lakso M, Sauer B, Mosinger B Jr, Lee EJ, Manning RW, Yu SH, Mulder KL, Westphal H., Targeted oncogene activation by site-specific recombination in transgenic mice.Proc Natl Acad Sci U S A. 1992 Jul 15;89(14):6232-6). This was in turn flanked by sequences homologous to exons 2 and 8 of a 110KB human BAC. Recombination resulted in the insertion to the floxed mCAT sequence between exons 2 and 8 of the BAC; this was used for conventional pronuclear injections.

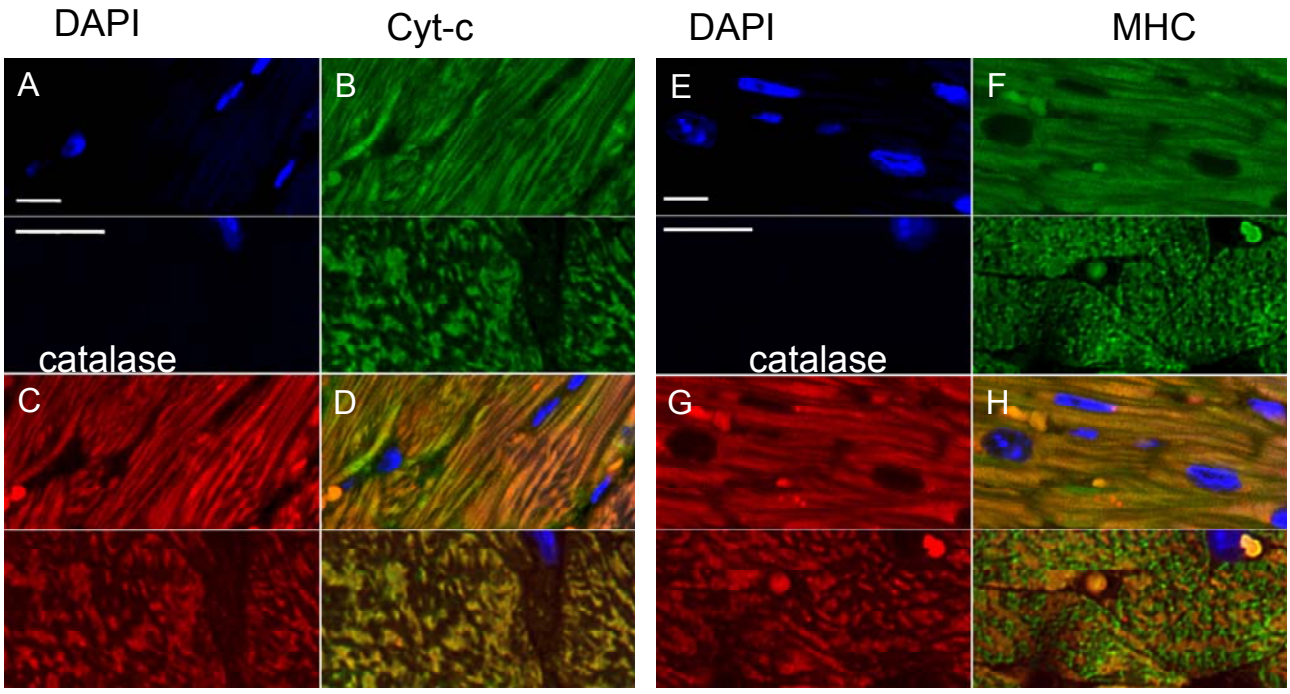

Online Figure II. Confocal micrographs of MHC-i-mCAT mouse hearts showing DNA (blue; A,E), human catalase (red; C,G), cytochrome C (green; B), myosin heavy chain (green; F) and composites of all three colors (D,H). Within each panel the top half shows cardiomyocytes at lower magnification and the bottom half shows cross-sectioned cardiomyocytes at higher magnification (bars=5 μm). At lower power, human catalase is found in cardiomyocytes co-stained with both cytochrome C (D) and myosin heavy chain (H), as shown by yellow colors. However, images at higher power illustrate that human catalase is co-localized with mitochondria (lower half of D), between myofilaments (lower half of H).

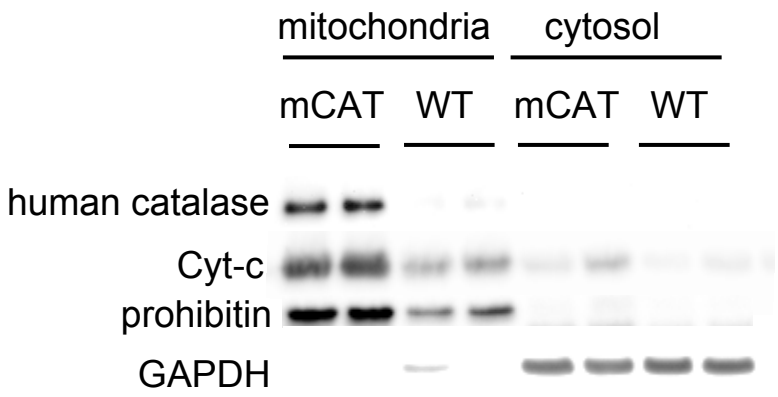

Online Figure III. Representative Western blot of cardiac mitochondrial and cytosolic fractions showing that only mitochondrial fraction of mCAT (human catalase targeted to mitochondria) but not the cytosolic fraction contained human catalase. Cytochrome-c and prohibitin were mainly found in the mitochondrial fraction and GAPDH was in the cytosolic fraction. Some contamination of the cytosolic fractions with mitochondrial proteins cytochrome-c and prohibitin is due to inadvertent disruption of mitochondria during cell lysis, however, human catalase is proportionally just as rare, or less so, in these fractions.

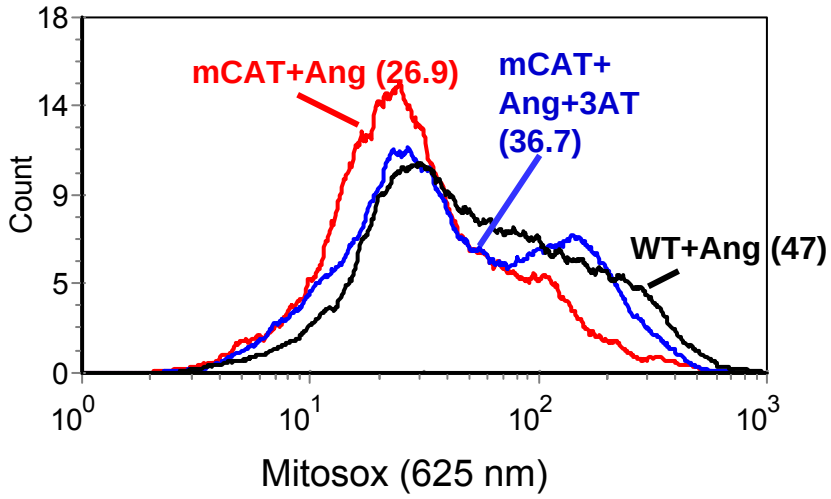

Online Figure .IV. The increase in mitochondrial ROS after Ang, detected by Mitosox fluorescence, was attenuated in mCAT cardiomyocytes, and this effect was abolished by pretreatment with 3 amino-triazole (3AT, 25mM), a catalase inhibitor. The medians of each histogram are presented in parenthesis

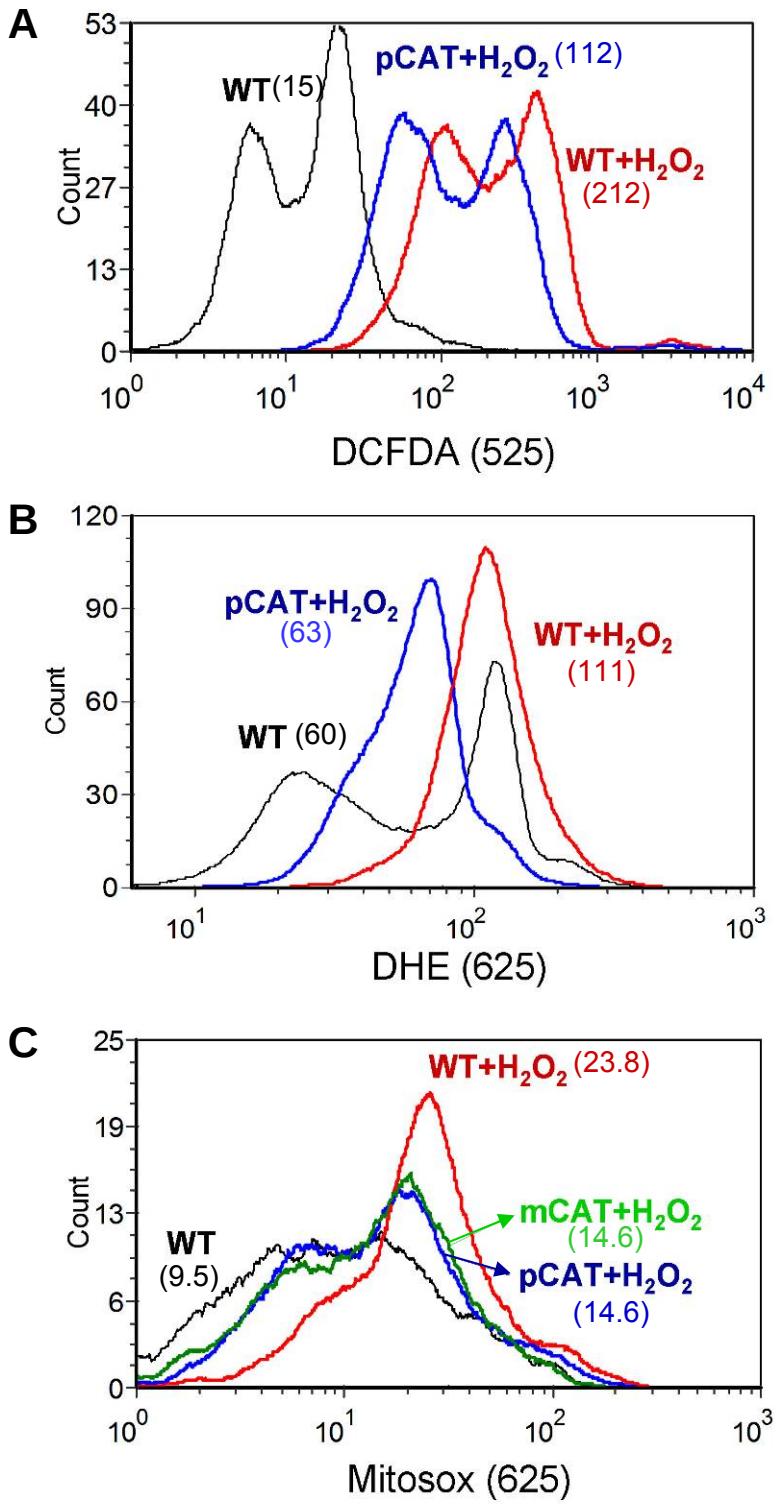

Online Figure V. Exogenous H_2O_2 (1mM) for 20 minutes markedly increase total cellular ROS, measured by DCFDA fluorescence (525 nm emission, A) or dihydroethidium fluorescence (625 nm emission, B) in WT neonatal mouse cardiomyocytes. Both measures of ROS were reduced by ~50% in pCAT cardiomyocytes. (C) H_2O_2 (0.2mM) for 40 minutes induced a significant increase in mitochondrial ROS (Mitosox fluorescence, 625 nm emission, C), and this was substantially reduced by the same extent in pCAT and mCAT cardiomyocytes. The median fluorescence intensity of each histogram is shown in parenthesis.

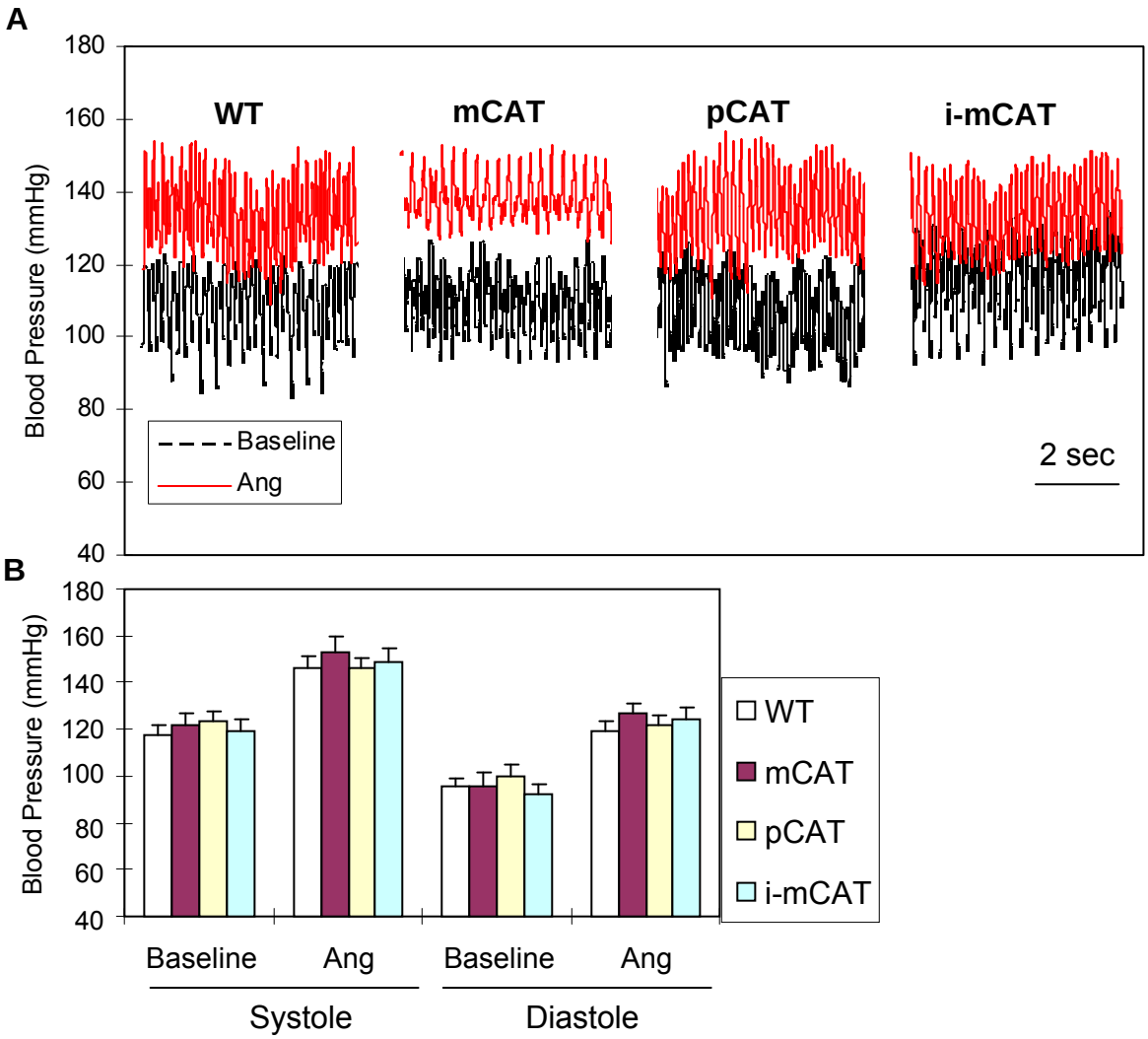

Online Figure VI. (A) Intravascular blood pressure monitoring by telemetry (Data Science International, DSI) demonstrated that continuous infusion of Angiotensin II (1.1mg/kd/d) increase systolic and diastolic blood pressure by approximately 25 mmHg in WT, mCAT, pCAT and MHC-i-mCAT mice. (B) WT, mCAT, pCAT and MHC-i-mCAT mice displayed a similar degree of systolic and diastolic blood pressure elevation after Ang.

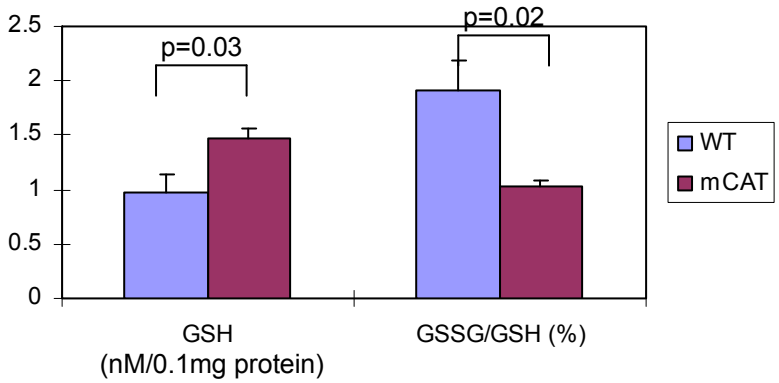

Online Figure VII. Glutathione levels in WT and mCAT hearts. Compared with WT mouse hearts, mCAT mouse hearts have a significantly higher level of GSH and a significantly lower ratio of GSSG/GSH, n=13-14. GSH and GSSG levels were measured using HPLC, as described[1]

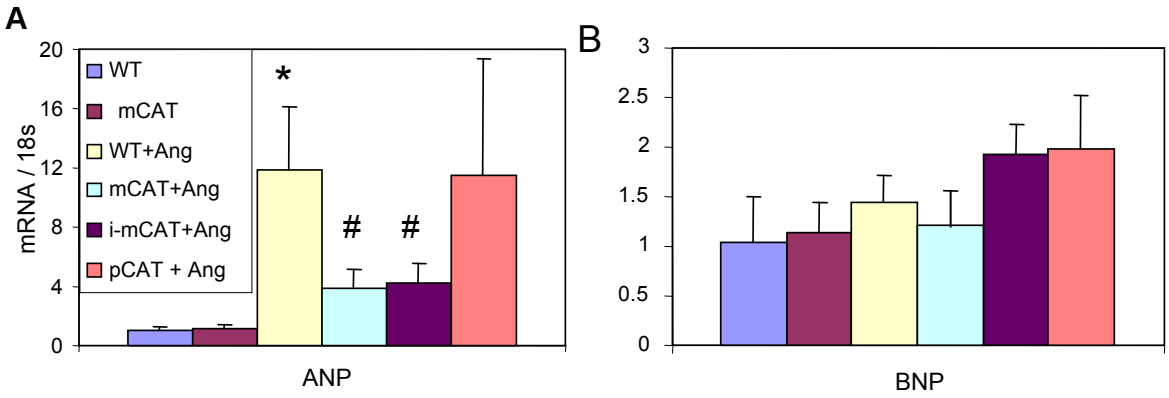

Online Figure VIII. Angiotensin II (Ang) significantly increased expression of ANP in WT mice, as quantified by qPCR, and this was attenuated equally by high (mCAT) or lower (MHC-i-mCAT) expression levels of mitochondrial, but not peroxisomal (pCAT) catalase. There was no significant change in BNP gene expression in any group. n=6-10 each group.

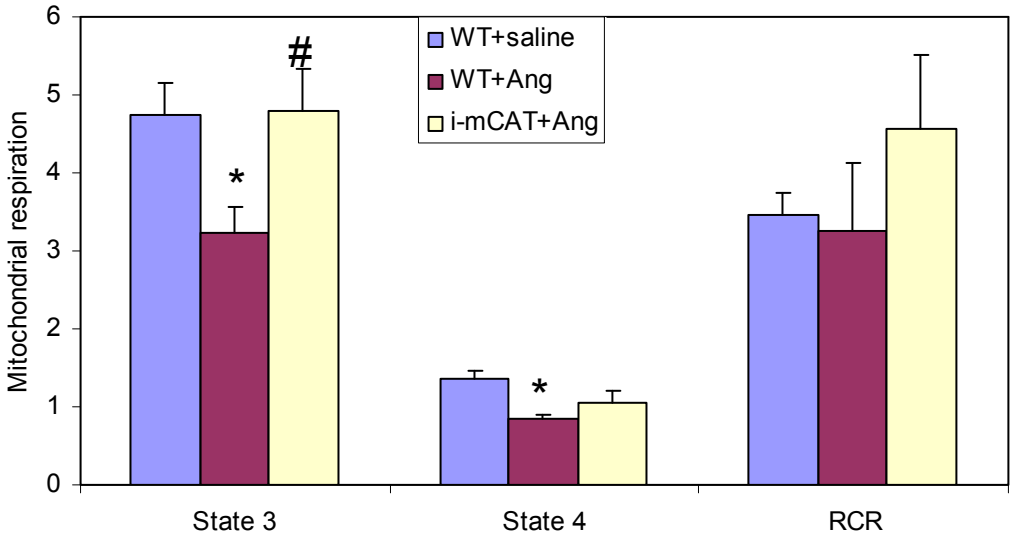

Online Figure IX. Ang-induced decline in mitochondrial state 3 (excess ADP, pyruvate and malate), state 4 (oligomycin treated) respiration (nmol O_2/min/mg) but not the RCR (respiratory control ratio = state 3 / state 4). The reduction in state 3 respiration is significantly attenuated by i-mCAT. The data is obtained using a Oxygraph-2K (Oroboros Instruments, Innsbruck, Austria), n=3-4, *$p<0.05$ between WT+saline vs. WT+Ang; $^{\#}p<0.05$ between WT+Ang vs. i-mCAT+Ang.

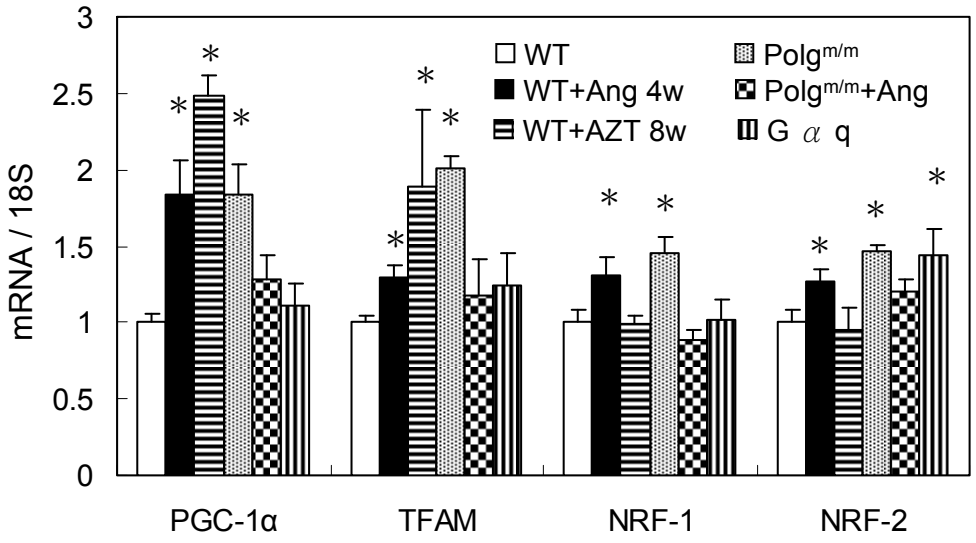

Online Figure X. Mitochondrial biogenesis in cardiac hypertrophy and failure. PGC-1α and its downstream target genes increased significantly in mice with cardiac hypertrophy (Ang or AZT treated mice and $Polg^{m/m}$ mice), but not in mice with heart failure (Ang treated $Polg^{m/m}$ or Gαq mice). *p<0.05 compared with WT. n=5-10.

Online Figure 11

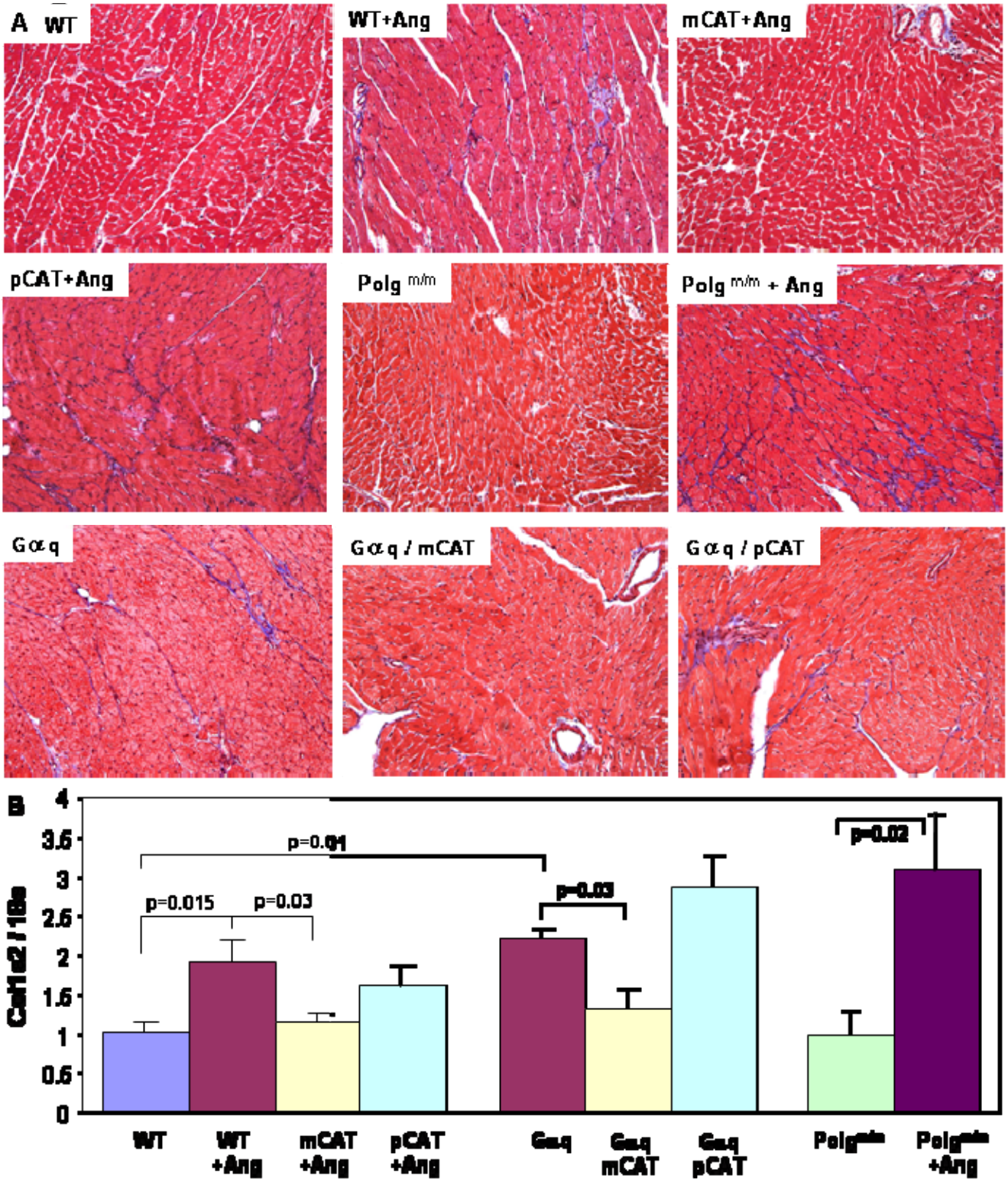

Online Figure XI Cardiac fibrosis. (A) Representative images of Masson`s trichrome staining of left ventricles showed that 4 weeks of Ang treatment or Gαq overexpression significantly induced cardiac fibrosis (blue) in WT mice, and that this was substantially attenuated in mCAT but not pCAT hearts. Polg$^{m/m}$ hearts have little fibrosis until treated with Ang (B). Procollagen type 1α2 expression was increased ~2 fold in hearts of mice treated with Ang or mice with Gαq overexpression, but this was attenuated in mCAT hearts; n=5-10 each group.

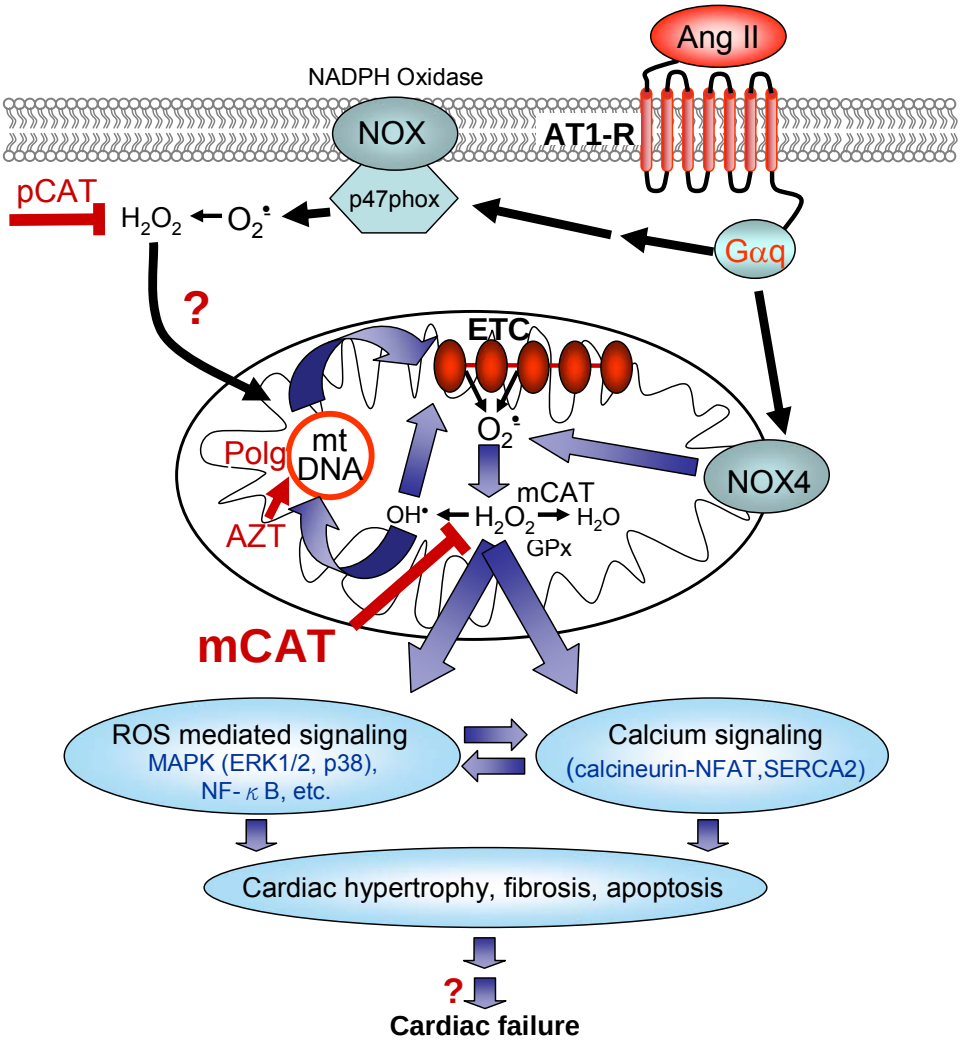

Online Figure XII. Hypothesized role of mitochondrial ROS in cardiac hypertrophy and failure. Experimental mouse models used in this study are shown in red. The relative contribution of membrane-bound NOX2 and mitochondrial associated NOX4 in cardiomyocytes is still unclear. Amplification of ROS within mitochondria appears to be required for Angiotensin II and G α q signaling. Primary damage to mtDNA from Polg and AZT is sufficient to cause cardiac hypertrophy/failure, which is also mediated by mtROS.

Online Table I. Genetic models used in this study

Genetic models	promoter	Strain	Notes	Ref.
Mitochondrial catalase (mCAT, 4033 lines)	chick beta-actin	C57Bl6 and 50% C3H, 50%C57Bl6	CMV enhancer, ~100 fold increase in total catalase activity in the heart	8
Rosa 26 i-mCAT	GAPDH-BAC	C57Bl6	floxed STOP is excised by Tamoxifen induced Rosa26 Cre. Low catalase expression (~2 fold increased activity)	
MHC i-mCAT	GAPDH-BAC	C57Bl6	floxed STOP is excised by Tamoxifen induced MHC-Cre. Cardiac specific, intermediate expression (~10 fold increased activity)	
Peroxisomal catalase (pCAT)	MHC	50% C57Bl6, 50%FVB (F1)	constitutive cardiac specific overexpression of wild-type (peroxisomal) catalase (~100 fold increased activity)	13
Gαq	MHC	50% C57Bl6, 50%FVB (F1)	Cardiac specific overexpression of 40 copies of Gαq, with 5 fold increased Gαq protein	15
Gαq / mCAT	MHC/ chick beta-actin	50% C57Bl6, 50% FVB (F2)		
Gαq / pCAT	MHC/ chick beta-actin	50% C57Bl6, 50% FVB (F2)		
$Polg^{m/m}$		C57Bl6	Homozygous AC→CT substitution at 1054-1055 of Polga results in D257A substitution which impairs the proofreading ability	18
$Polg^{m/m}$ / mCAT		C57Bl6		

Online Table II. Body and organ weights (mean±SEM)

Experiment	Groups	Age (months)	n	Body wt (g)	Heart wt (mg)	Tibia (mm)	Heart wt/ tibia	Lung wt (mg)	Lung wt/ tibia
pCAT	WT+Saline	4	3	29.7±1.7	126±6.7	23.3±0.6	5.39±0.13		
	pCAT+Saline	4	3	31.4±1.3	132±1.5	23.8±0.3	5.54±0.12		
	WT+Ang	4	4	29.9±1.3	160±8.8	22.3±0.3	7.14±0.48*		
	pCAT+Ang	4	6	31.4±0.5	161±4.2	23.1±0.3	6.99±0.18		
mCAT (4033) C57Bl6	WT+Saline	3	3	29.8±1.5	123±5.7	23.8±0.7	5.17±0.14		
	mCAT+Saline	3	3	30.5±0.9	124±8.8	23.9±0.9	5.18±0.28		
	WT+Ang	3	4	32.6±2.0	183±9.3	24.5±0.4	7.45±0.38**		
	mCAT+Ang	3	4	28.9±0.2	148±4.8	23.8±0.2	6.24±0.17†		
MHC-i-mCAT	WT+Saline	3	3	28.1±0.8	127±5.8	23.9±0.7	5.31±0.15		
	mCAT+Saline	3	3	27.5±0.4	125±7.2	23.6±0.6	5.27±0.21		
	WT+Ang	3	6	28.7±1.9	170±7.2	23.6±0.6	7.22±0.23**		
	mCAT+Ang	3	6	26.9±0.5	152±7.5	24.0±0.7	6.31±0.18††		
R26-i-mCAT	WT+Saline	6	3	32.5±0.9	148±9.6	25.5±0.5	5.79±0.28		
	mCAT+Saline	6	3	33.0±0.7	145±8.7	25.5±0.6	5.68±0.32		
	WT+Ang	6	6	34.2±0.7	210±9.7	25.2±0.3	8.35±0.37**		
	mCAT+Ang	6	7	34.0±0.7	182±8.2	25.6±0.3	7.11±0.26†		
Gαq	WT	4	3	29.1±1.8	135±4.8	23.2±0.2	5.82±0.18	144±5.7	6.20±0.14
	Gαq	4	5	28.7±1.2	180±7.3	23.1±0.3	7.77±0.24**	175±3.2	7.54±0.08**
	Gαq/mCAT	4	5	26.8±1.6	136±7.8	23.2±0.1	5.87±0.26††	153±8.0	6.57±0.27†
	Gαq/pCAT	4	5	27.6±2.5	178±6.9	22.8±0.1	7.80±0.31	176±6.3	7.73±0.29
Mitochondrial mutator	WT	4	3	28.6±0.5	130±3.8	23.0±0.5	5.61±0.29	138±5.4	6.0±0.18
	$Polg^{m/m}$	4	3	28.1±0.4	164±1.9	22.7±0.3	7.22±0.16**	138±4.2	6.11±0.29
	$Polg^{m/m}$+Ang	4	7	27.4±1.0	176±11.3	22.9±0.1	7.66±0.49**	217±22.6	9.47±0.76**
	$Polg^{m/m}$/mCAT+Ang	4	4	26.9±1.2	169±4.7	23.1±0.1	7.34±0.20	175±3.8	7.58±0.13†

*p<0.05, **p<0.01 compared with WT± saline controls in the same experiment, †p<0.05, ††p<0.01 mCAT compared with the non-mCAT littermates.

Online Table III. Echocardiographic measurements (mean±SEM) of mCAT4033 (high expressor), R26-i-mCAT (low expressor), cardiac specific pCAT and mCAT male mice, together with its own WT littermate controls, before and after Ang for 4 weeks

Group	Genotype	Strain	n	Ang	M-mode					Tissue Doppler
					IVS (mm)	LVPW (mm)	LVEDD (mm)	LVESD (mm)	FS%	Ea/Aa
pCAT	WT	50% C57Bl6, 50% FVB	4	Pre-	0.97± 0.03	1.03± 0.03	2.80± 0.10	1.37± 0.09	51.0± 1.9	1.36± 0.09
				Post-	1.37± 0.09	1.40± 0.10	2.80± 0.12	1.30± 0.17	52.7± 2. 7	0.84± 0.02
				Change¶	*1.41±0.05*	*1.35±0.09*	*1*	*0.96±0.15*	*1.039±0.09*	*0.57±0.06*
	pCAT		6	Pre-	1.00± 0.03	1.03± 0.04	2.90± 0.04	1.53± 0.06	48.7± 2.1	1.20± 0.07
				Post-	1.35± 0.02	1.33± 0.03	2.85± 0.03	1.40± 0.06	52.9± 1.3	0.86± 0.10
				Change	*1.35±0.04*	*1.30±0.07*	*0.98±0.02*	*0.64±0.21*	*1.11±0.05*	*0.74±0.11*
mCAT (4033)	WT	C57Bl6	4	Pre-	0.88± 0.05	0.88± 0.06	3.00± 0.11	1.53± 0.05	51.7± 1.0	1.49± 0.11
				Post-	1.25± 0.13	1.20± 0.04	3.20± 0.07	1.40± 0.08	54.9± 1.3	0.87± 0.19
				Change	*1.45±0.10*	*1.38±0.06*	*1.06±0.06*	*0.90±0.08*	*1.06±0.02*	*0.57±0.09*
	mCAT		6	Pre-	1.00± 0.05	1.06± 0.03	2.77± 0.07	1.53± 0.07	47.6± 1.9	1.52± 0.18
				Post-	1.01± 0.03	1.10± 0.06	2.87± 0.09	1.30± 0.10	55.3± 1.5	**1.29± 0.06***
				Change	***1.07±0.03****	***1.03±0.03****	*1.04±0.04*	*0.85±0.03*	*1.19±0.04*	*0.87±0.11*
mCAT (4033)	WT	50% C3H, 50% C57Bl6	6	Pre-	0.83± 0.05	0.83± 0.05	3.43± 0.11	1.65± 0.04	51.3± 1.7	1.49± 0.11
				Post-	1.3± 0.05	1.23± 0.06	3.57± 0.05	1.95± 0.10	48.9± 2.2	1.08± 0.21
				Change	*1.61±0.15*	*1.38±0.06*	*1.04±0.03*	*1.18±0.05*	*0.95±0.04*	*0.73±0.13*
	mCAT		6	Pre-	0.87± 0.02	0.77± 0.06	3.58± 0.08	1.83± 0.09	48.6± 2.3	1.43± 0.09
				Post-	0.97 ± 0.06	0.87± 0.04	3.42± 0.15	1.68± 0.10	49.3± 2.2	1.41± 0.07
				Change	***1.12±0.08****	***1.16±0.09****	*1.01±0.04*	***0.93±0.08****	*1.03±0.07*	*1.02±0.09*
MHC-imCAT	WT	C57Bl6	6	Pre-	0.97± 0.04	0.96± 0.04	3.10± 0.11	1.60± 0.07	48.7± 2.0	1.28± 0.04
				Post-	1.30± 0.08	1.27± 0.09	3.30± 0.15	1.56± 0.09	49.7± 1.4	0.85± 0.05
				Change	*1.34±0.07*	*1.35±0.09*	*1.05±0.05*	*0.99±0.10*	*1.03±0.05*	*0.67±0.03*

				Pre-	0.97± 0.03	0.97± 0.06	2.90± 0.10	1.40± 0.10	51.5± 1.9	1.32± 0.09
	mCAT		6	Post-	1.08± 0.03	1.01± 0.07	2.90± 0.11	1.42± 0.07	51.5± 1.0	**1.20± 0.14***
				Change	***1.13±0.06****	***1.03±0.06****	*1.02±0.02*	*1.01±0.05*	*1.00±0.03*	*0.93±0.08*
				Pre-	0.97± 0.04	0.95± 0.06	3.18± .011	1.60± 0.09	49.0± 2.3	1.29± 0.04
	WT		6	Post-	1.28± 0.09	1.18± 0.16	3.31± 0.18	1.57± 0.11	49.0± 1.4	0.85± 0.06
R26-imCAT		C57Bl6		*Change*	*1.33±0.08*	*1.27±0.19*	*1.04±0.06*	*1.00±0.11*	*1.01±0.05*	*0.66±0.04*
				Pre-	1.07± 0.04	0.86± 0.06	3.35± 0.07	1.68± 0.07	49.7± 1.5	1.44± 0.07
	mCAT		7	Post-	1.15± 0.06	1.03± 0.08	3.30± 0.08	1.45± 0.10	55.3± 2.0	**1.34±0.13****
				Change	***1.08±0.05****	*1.50±0.09*	*0.98±0.02*	*0.85±0.09*	*1.12±0.06*	***0.92±0.07****

¶ Fold changes = post-Ang / pre-treatment group

*p<0.05 for transgenic (mCAT) vs. WT littermates comparison

**p<0.01 for transgenic (mCAT) vs. WT littermates comparison

IVS: interventricular septum, LVPW: LV posterior wall, EDD and ESD: End-diastolic and End-systolic diameter, respectively